

A NEW VHF DOPPLER RADAR EXPERIMENT AT SYOWA STATION, ANTARCTICA

Kiyoshi IGARASHI,

Radio Research Laboratories, 2-1, Nukui-Kitamachi 4-chome, Koganei-shi, Tokyo 184

Tadahiko OGAWA,

*Hiraiso Branch, Radio Research Laboratories, 3601 Isozaki,
Nakaminato-shi, Ibaraki 311-12*

Masami OSE,

Radio Research Laboratories, 2-1, Nukui-Kitamachi 4-chome, Koganei-shi, Tokyo 184

Ryoichi FUJII and Takeo HIRASAWA

National Institute of Polar Research, 9-10, Kaga 1-chome, Itabashi-ku, Tokyo 173

Abstract: A new VHF doppler radar with a minicomputer for real-time processing and radar control will be operational in 1982 at Syowa Station, Antarctica, in order to study *E*-region irregularities and neutral wind motions. This project, one of the ground-based study programs in Antarctica for the Middle Atmosphere Program (MAP, 1982-1985), aims at clarifying how the middle atmosphere in the 80-110 km altitude region behaves in response to the energy flow from the magnetosphere into the polar ionosphere, especially during a substorm. The radar has three operation modes; spectrum mode, double-pulse mode and meteor mode. The spectrum mode provides doppler spectra of back-scattered signals from which characteristics of the plasma turbulence due to auroral activity can be investigated. Mean drift velocities of the irregularities are derived from the double-pulse mode. The drift velocity obtained by this mode ultimately can be related to the ionospheric electric field. In the meteor mode, wind motions in the 80-110 km altitudes are investigated by using meteor trails.

1. Introduction

The Syowa Station auroral radar capable of measuring only the intensity of radio auroral echoes is being now operated at 50, 65, 80 and 112 MHz. This radar was modified in 1977 to study the spectral form and drift velocity of the irregularities. Preliminary results of the spectral characteristics and irregularity production mechanisms obtained by the modified radar have been reported elsewhere (IGARASHI *et al.*, 1981; OGAWA and IGARASHI, 1982). Recently, it has become clear that the doppler signature of 50 MHz backscatter echoes from radio aurora is closely related to the *E*-region plasma drift velocity and that VHF doppler radar is a useful diagnostic tool for the auroral zone studies (ECKLUND *et al.*, 1977; GREENWALD *et al.*, 1978; CHAILL *et al.*, 1978; OGAWA *et al.*, 1982). In this connection, the development of a new radar was

started in 1980 as a joint project between the Radio Research Laboratories and the National Institute of Polar Research.

The new VHF doppler radar is designed to provide high spatial and time resolution measurements of the intensity and doppler velocity of radar auroral irregularities. It has the radar beams directed toward geomagnetic south (GMS) and geographic south (GGS) to investigate the two-dimensional structure of the irregularities. Echo signals are processed by an on-line minicomputer. Intensity, power spectra and mean doppler velocity of the echoes are stored on digital magnetic tapes.

This radar also can detect a meteor echo in the 90–110 km height region and determine in real-time the range, height and doppler shift of the echo (Aso *et al.*, 1979). The upper atmospheric wind measurement by this radar will be the second in Antarctica since an equipment for measuring winds in the height region of 80–100 km was previously operated at Mawson Base (ELFORD and MURRAY, 1960).

2. Equipments

Some parameters pertinent to the present radar system are listed in Table 1. The system block diagram is shown in Fig. 1. The radar is a coherent pulse type using narrow-beam antennas and on-line data processing and recording equipments. The radar is fully controlled by a minicomputer system (MELCOM, model 70/25) consisting of a 96 K byte memory, FFT processor (MSP-2), floppy disk, console typewriter, graphic display and two magnetic tape units.

The radar frequencies are 50 and 112 MHz, of which the latter frequency will be available in 1983. A transmitter pulse width is variable from 10 μ s to 100 μ s in 10 μ s steps. A pulse compression (13 bit Barker-code modulation with a 10 μ s sub-pulse length) is also possible for getting signal-to-noise ratio and range resolution higher than the normal pulse-modulation. The pulse repetition frequency (PRF) is also

Table 1. Parameters of the VHF doppler radar.

Site	Syowa Station, Antarctica (69°00'S, 39°35'E)
Type	Coherent pulse radar
Frequency	50, 112 MHz
Peak power	~ 15 kW
Pulse width	10 μ s ~ 100 μ s (10 μ s step) 130 μ s (10 μ s \times 13 bits); Barker-code modulation
PRF	50 Hz ~ 400 Hz (1 Hz step)
Antenna	Three 14-element coaxial collinear (two-way)
Antenna gain	25 dB
Antenna beamwidth	3° ~ 4° (half power) in horizontal plane
Receiver bandwidth	Matched to pulse width
Data processing	On-line minicomputer (MELCOM 70/25)
Operation mode	1. Spectrum mode for radio aurora 2. Double-pulse mode for radio aurora 3. Meteor mode for meteor trail

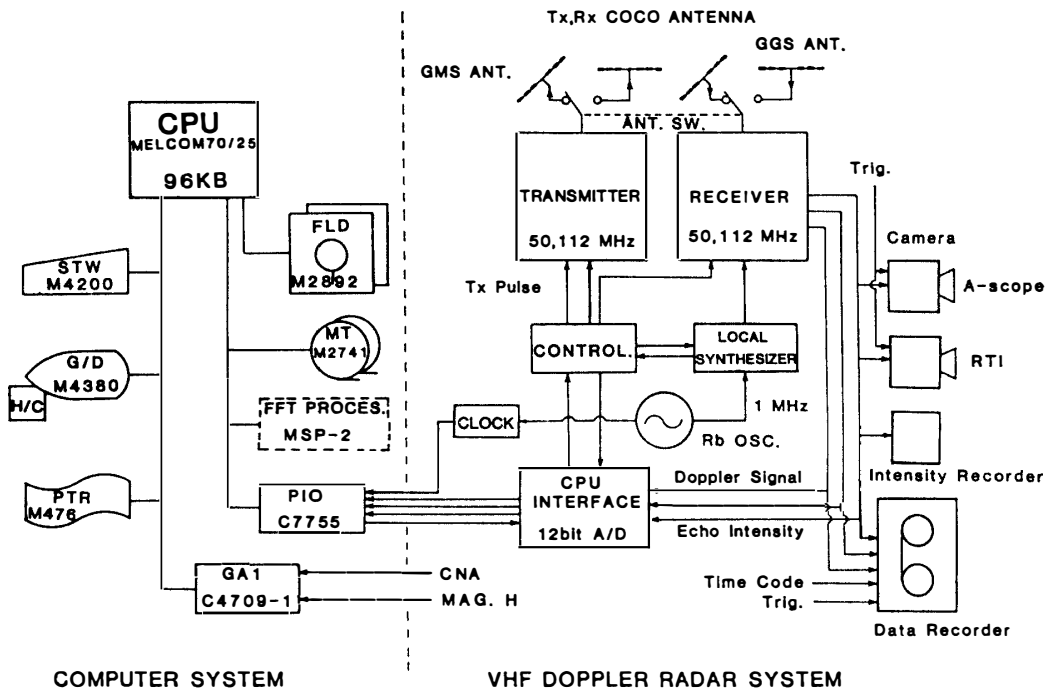


Fig. 1. Block diagram of the VHF doppler radar and computer systems. Four identical coaxial-collinear antennas directing geomagnetic south (GMS) and geographic south (GGS) are used for transmitting and receiving. The transmitting antenna is connected to a 15-kW peak power transmitter. The radar system is operated under the control of the mini-computer.

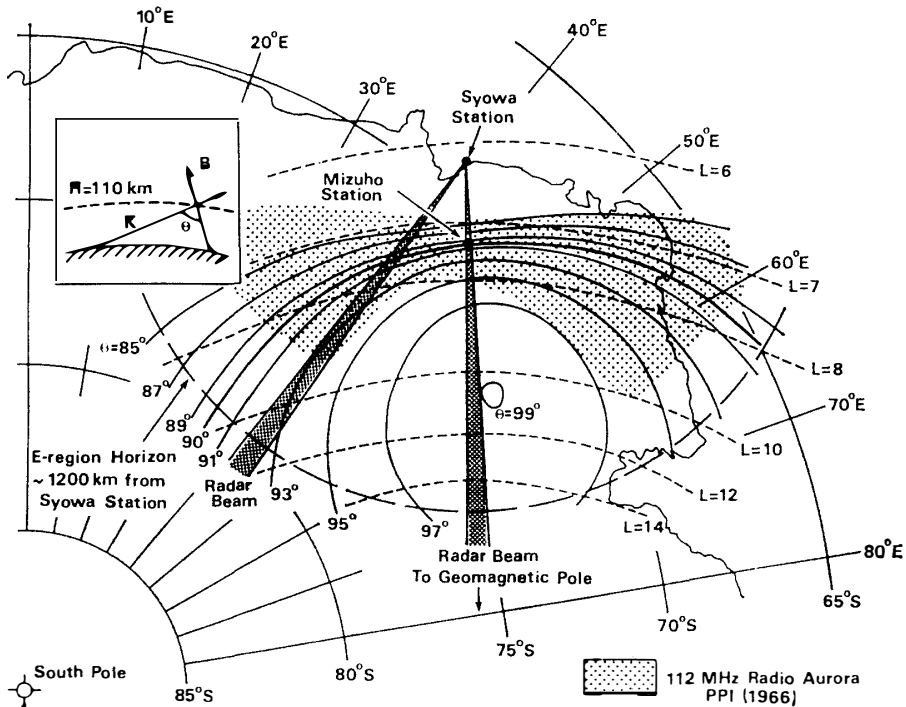


Fig. 2. Plan view of radar antenna patterns together with contours of L values and aspect angles θ . The aspect contours are shown for a height of 110 km. The dotted-area represents the region of 112 MHz radio aurora recorded by PPI.

variable from 50 Hz to 400 Hz in 1 Hz steps. The peak power of the transmitter is about 15 kW.

Analog signals received are converted to digital signals by 12 bit A/D converters and then transferred to the computer system for processing and recording. The power spectra of backscattered signals are calculated by the FFT processor and then stored on magnetic tapes. Mean doppler velocity is obtained by calculating the phase quadrature outputs from the receiver according to the mean doppler algorithm described by RUMMER (1968). The system also can detect the parameters related to meteor echoes.

The plan view of the two antenna beams is shown in Fig. 2 together with the magnetic L -shell and aspect angle (θ defined in the figure) contours. The beams are directed to geomagnetic south (GMS) and to geographic south (GGS). Note that the GGS beam can cover a more extended region than the GMS beam as inferred from the echoing area measured by the 112 MHz PPI (Plane Position Indication) technique. Each beam, having a beamwidth of 3° to 4° in the horizontal plane, is formed by using three 14-element coaxial collinear antennas (BALSLEY and ECKLUND, 1972a).

3. Data Processing

3.1. Power spectrum mode

The power spectrum of backscattered signals is obtained by the method described by BALSLEY and ECKLUND (1972b). The time chart of data sampling is shown in Fig. 3. The phase quadrature outputs (A and B channels) and the backscattered power (P channel) from the phase coherent receiver are sampled every $100 \mu\text{s}$ by the 12 bit A/D converter. The Fourier transformation is continuously executed by the FFT

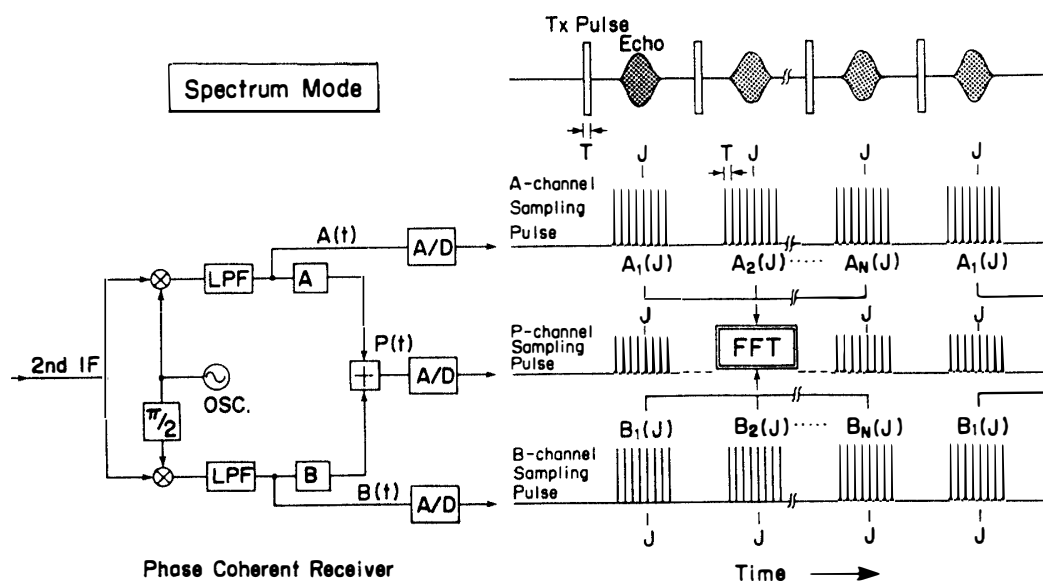


Fig. 3. Time chart of data sampling for the spectrum mode. As shown, the quadrature outputs from the phase coherent receiver are digitized and then stored in the buffer-memory in the computer for power spectrum analysis by the FFT processor. The pulse repetition frequency is typically 300 to 400 Hz. T is typically $100 \mu\text{s}$.

processor (MSP-2 array processor). The power level from a given echo-range is given by the expression:

$$P(J) = A^2(J) + B^2(J) \quad (1)$$

where $A(J)$ and $B(J)$ are the quadrature outputs for range J . The complex Fourier transformations of $A(t)$ and $B(t)$ are calculated as

$$A(t) \leftrightarrow R_A(J) + iI_A(J) \quad (2)$$

$$B(t) \leftrightarrow R_B(J) + iI_B(J) \quad (3)$$

where the sign \leftrightarrow implies the transformation process. The power components at the J -th frequency above and below the transmitted frequency, $S(J)$ and $S(-J)$, respectively, are given by the expressions:

$$S(J) = R^2(J) + I^2(J) \quad (4)$$

$$S(-J) = R^2(-J) + I^2(-J) \quad (5)$$

where

$$R(J) = (R_A(J) + I_B(J))/2 \quad (6)$$

$$R(-J) = (R_A(J) - I_B(J))/2 \quad (7)$$

$$I(J) = (I_A(J) - R_B(J))/2 \quad (8)$$

$$I(-J) = -(I_A(J) + R_B(J))/2 \quad (9)$$

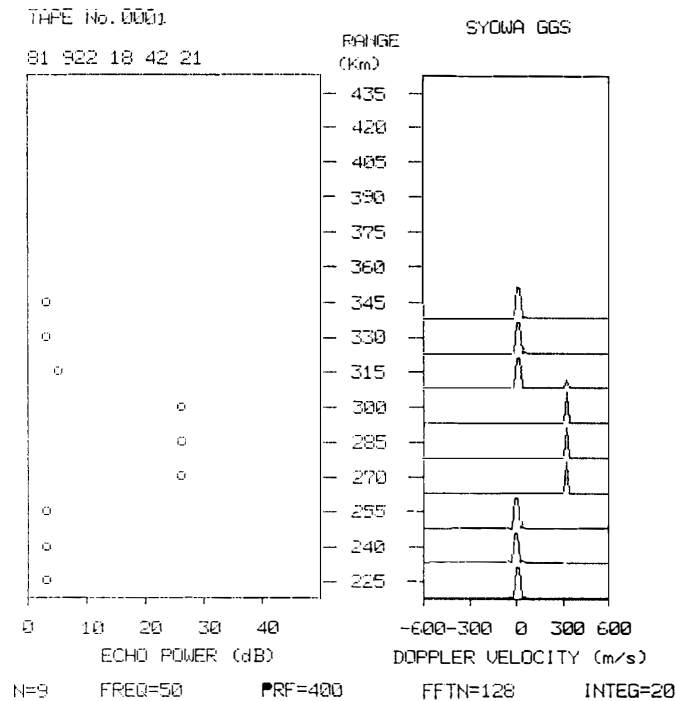


Fig. 4. Range profiles of echo intensity (left) and power spectrum (right) of a test-signal processed by the computer for the spectrum mode. The doppler velocity of the test-signal is 300 m/s. The spectrum was obtained by using a 128-point FFT and by averaging twenty spectra over 6.4 s. Note that the spectra appearing around the Doppler velocity of zero are not real and should be neglected.

$P(J)$, $S(J)$ and $S(-J)$ are averaged over an integration time. A quick-look display after the computer processing of a test signal is shown in Fig. 4.

3.2. Double pulse mode

In the double-pulse mode, single pulse and double pulses (pulse separation of τ) are emitted alternately as shown in Fig. 5. Echo power is obtained from the P channel for the single pulse. On the other hand, the mean doppler velocity of the irregularities is obtained from the double-pulse echoes by applying the method similar to that used in the STARE radar in operation in Scandinavia (GREENWALD *et al.*, 1978). The phase quadrature outputs (A and B channels) from the phase coherent receiver are sampled twice with a time separation of τ as shown in Fig. 5. The real and imaginary parts of the double-pulse autocorrelation coefficient are calculated from the quadrature samples of $A(J)$ and $B(J)$ as follows:

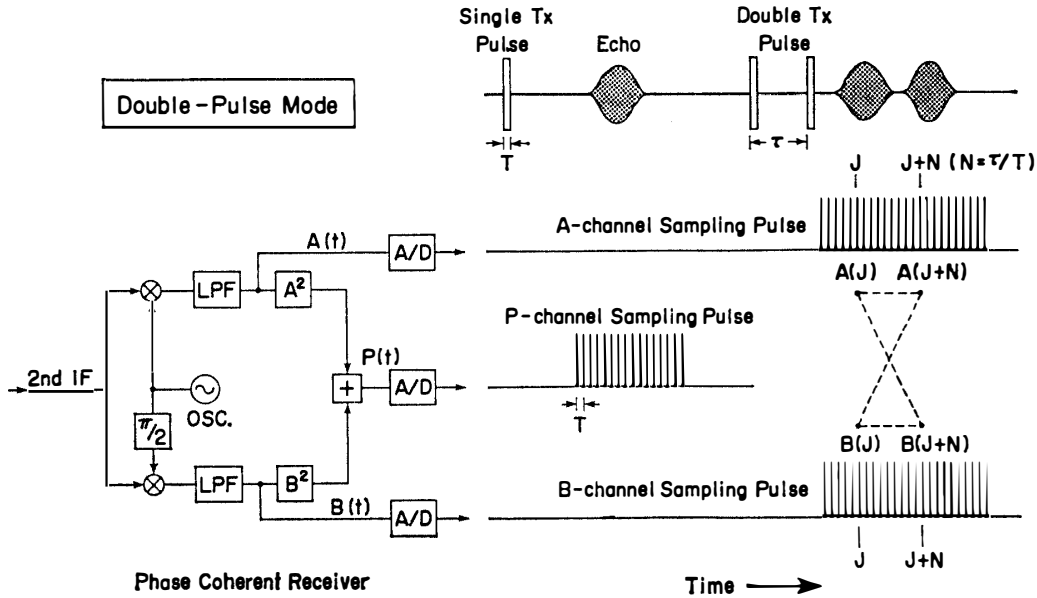


Fig. 5. Time chart of data sampling for the double-pulse mode. T is a transmitting pulse width (typically $100 \mu\text{s}$) and τ is a double-pulse separation (typically 1.5 ms). The quadrature outputs from the phase coherent receiver are processed by the computer to obtain the auto-correlation coefficient.

$$R(J) = A(J)A(J+N) + B(J)B(J+N) \quad (10)$$

$$I(J) = A(J+N)B(J) - A(J)B(J+N) \quad (11)$$

where NT equals to τ , T being the time separation between two samplings. In our case, τ is 1.5 ms and T is $100 \mu\text{s}$. After averaging $R(J)$ and $I(J)$ over 20 s, the mean phase shift of the irregularities at range J during the time interval of τ is calculated as

$$\bar{\phi}(J) = \tan^{-1} [I(J)/R(J)]. \quad (12)$$

Then, the mean doppler velocity is given by

$$V(J) = (\lambda/4\pi\tau)\bar{\phi}(J) \quad (13)$$

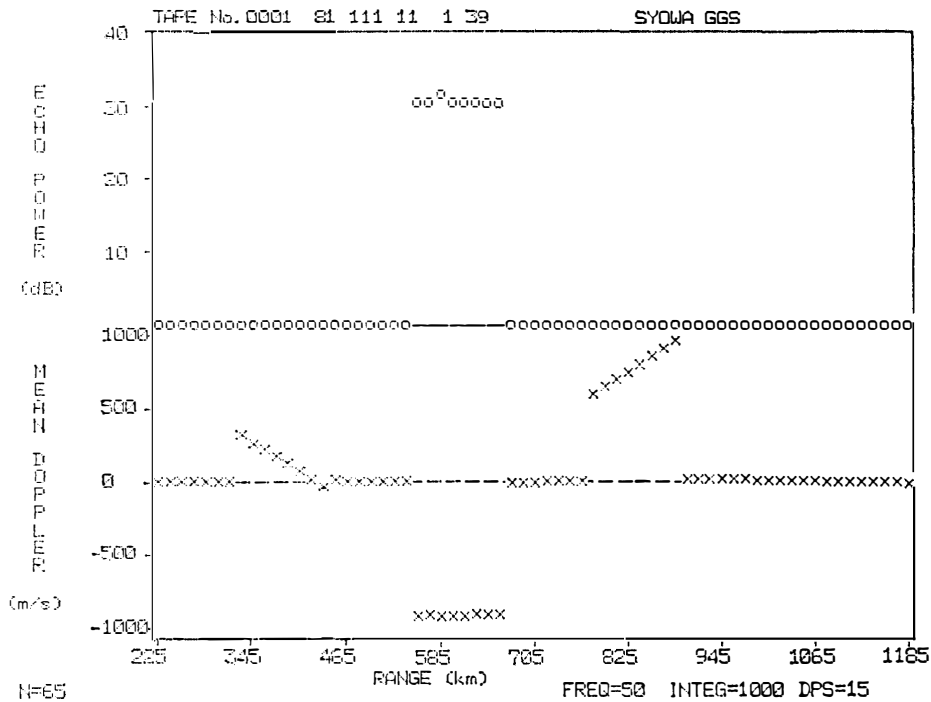


Fig. 6. Range profiles of echo intensity (upper) and mean doppler velocity (lower) of a test-signal processed by the computer for the double-pulse mode. The doppler velocity of the test-signal is 900 m/s and the double-pulse separation is 1.5 ms. The integration time to get one profile is 20 s.

where λ is the radar wavelength. A quick-look display after the computer processing of a test signal is shown in Fig. 6.

3.3. Meteor mode

The previous Syowa Station radar detected not only radio aurora but also a number of meteor echoes. An example of an A-scope film record (multiple exposure) of the meteor echoes is shown in Fig. 7. The pulse repetition frequency in this example is 50 Hz. In Fig. 7, the weak auroral echoes are seen at the ranges of 250–300 km and the sharp meteor echoes appear at 280 km. The echo power due to a meteor drops exponentially with time as shown at the right side. The time chart of data sampling for the meteor mode is shown in Fig. 8. In the case of real-time processing by a computer, it may be difficult to distinguish a meteor echo from radio aurora when both echoes appear simultaneously. To pick up only the meteor echo and process it by the computer, the following method is adopted here. The range extent of radio aurora is usually wider than that of meteor echo. Relying on this fact, if the echo width in range is shorter than or comparable to the transmitter pulse width and also if the echo power is beyond the threshold strength, the 'flag' signal (designated as 'interrupt' in Fig. 8) is sent from the receiver to the computer. After receiving the interrupt signal, the computer determines the echo range with a time resolution of $1 \mu\text{s}$ and begins to sample every $200 \mu\text{s}$ for 1 s the doppler signal and echo intensity at the particular range. The line-of-sight velocity of the echo trail is calculated from the doppler signal channel having an offset frequency of f_0 by using the so-called

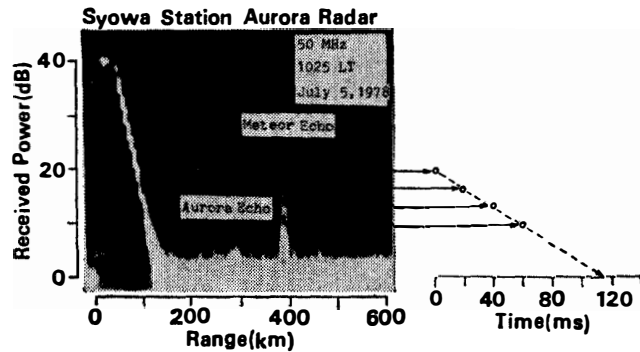


Fig. 7. A-scope film record of meteor echo observed by the 50 MHz auroral radar at Syowa Station in 1978. The meteor echo decays exponentially with time. The radio aurora echo is seen around 280 km range.

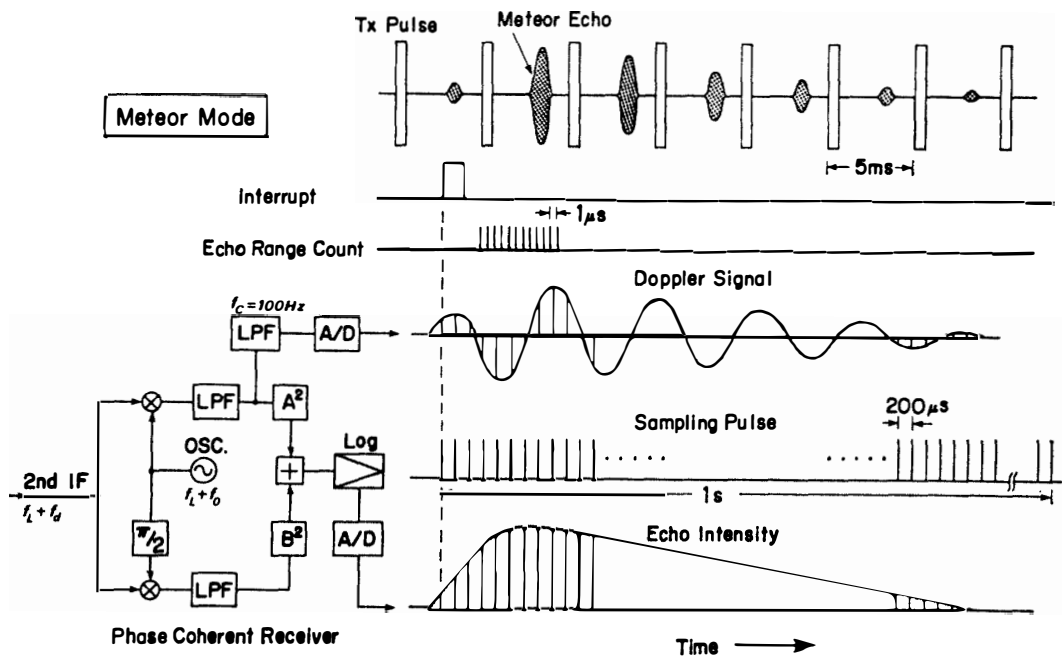


Fig. 8. Time chart of data sampling for the meteor mode. The interrupt signal to the computer is generated as soon as meteor echo is identified. Then, the computer begins to count the echoing range and to store the doppler signal and echo intensity every 200 μs for 1 s.

zero-crossing method. The echo amplitude decay time T_{un} for an under-dense trail is given by

$$T_{un} = \lambda^2 / 16\pi^2 D \tag{14}$$

where D is the ambipolar diffusion coefficient. T_{un} is determined by a least-mean-square method. The echo height, $H(\text{km})$, is derived from the following relation (MCKINLEY, 1961);

$$\log_{10} D = 0.067H - 5.6 \tag{15}$$

The digitized doppler signals and echo intensities at 500 sampling-points (corresponding to a time interval of 100 ms) are stored on magnetic tapes with the diffusion coef-

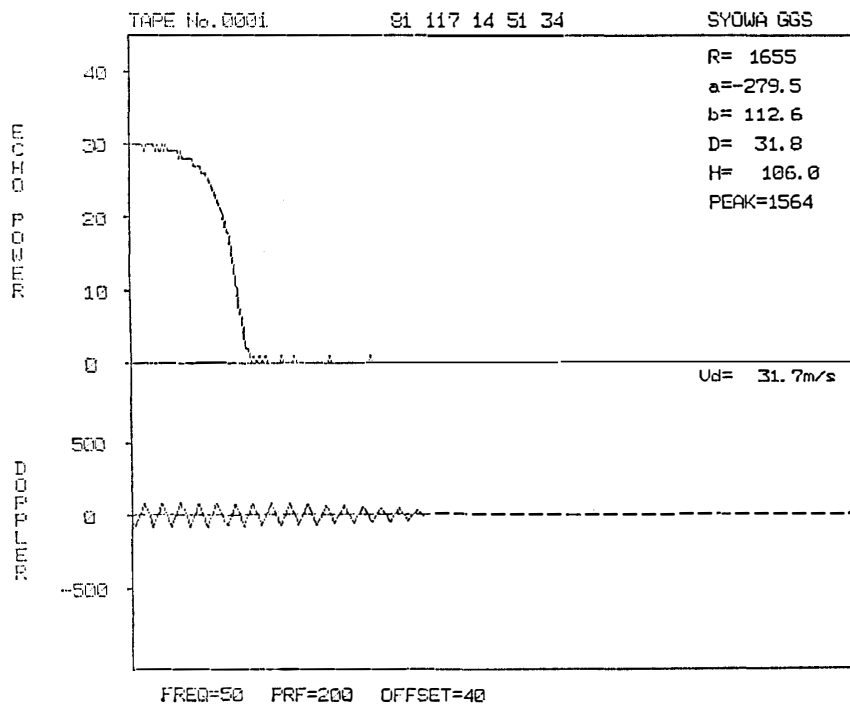


Fig. 9. Time profiles of echo power (upper) and doppler signal (lower) stored in the computer for the meteor mode. Full scale length of the abscissa is 100 ms. Also shown are the echo range (R in μs), diffusion coefficient (D in m^2/s), echo height (H in km), peak echo-intensity (PEAK in digit, full scale is 2047) and doppler velocity (V_a in m/s).

ficient, echo height and echo range.

A quick-look display after the computer processing of a test signal is shown in Fig. 9.

4. Concluding Remarks

The new radar system will begin operation early in 1982. The three observational modes described in Section 3 are used separately in the experiment. The double pulse mode is used to survey entire pictures of radio aurora. Fine structures of the irregularities are distinguished from the spectrum mode. The probing antenna can be alternately switched to geographic and to geomagnetic south for the above two modes. The meteor mode which detects neutral wind motions in the 80–110 km height region will be operated primarily in the IAGA CTOP (Cooperative Tidal Observation Program) campaign periods.

The data stored on magnetic tapes at Syowa Station will be analyzed later in detail after the wintering party comes back to Japan.

Acknowledgments

We thank Drs. Y. HAKURA and R. MAEDA and Mr. Y. KURATANI of the Radio Research Laboratories for their kind support to this project.

References

- ASO, T., TSUDA, T. and KATO, S. (1979): Meteor radar observation at Kyoto University. *J. Atmos. Terr. Phys.*, **41**, 517–525.
- BALSLEY, B. B. and ECKLUND, W. L. (1972a): A portable coaxial collinear antenna. *IEEE Trans.*, **AP-20**, 513–516.
- BALSLEY, B. B. and ECKLUND, W. L. (1972b): VHF power spectra of the radar aurora. *J. Geophys. Res.*, **77**, 4746–4760.
- CAHILL, L. T., GREENWALD, R. A. and NIELSEN, E. (1978): Auroral radar and rocket double probe observations of electric field across the Harang discontinuity. *Geophys. Res. Lett.*, **5**, 687–690.
- ECKLUND, W. L., BALSLEY, B. B. and CARTER, D. A. (1977): A preliminary comparison of *F*-region plasma drifts and *E*-region irregularity drifts in the auroral zone. *J. Geophys. Res.*, **82**, 195–197.
- ELFORD, W. G. and MURRAY, E. L. (1960): Upper atmosphere wind measurements in the Antarctic. *Space Res.*, **1**, 158–163.
- GREENWALD, R. A., WEISS, W., NIELSEN, E. and THOMSON, N. R. (1978): STARE; A new radar auroral backscatter experiment in northern Scandinavia. *Radio Sci.*, **13**, 1021–1039.
- IGARASHI, K., OGAWA, T., TSUZURAHARA, S., SHIRO, I., OSE, M. and YAMAGISHI, H. (1981): Simultaneous observations of aurora with a doppler-radar and sounding rockets. *Mem. Natl Inst. Polar Res., Spec. Issue*, **18**, 391–402.
- IGARASHI, K. and TSUZURAHARA, S. (1981): Spatial correlations between radio aurora and 4278Å aurora intensity. *Mem. Natl Inst. Polar Res., Spec. Issue*, **18**, 204–211.
- MCKINLEY, D. W. R. (1961): *Meteor Science and Engineering*. New York, McGraw-Hill.
- OGAWA, T. and IGARASHI, K. (1982): VHF radar observation of auroral *E*-region irregularities associated with moving-arcs. *Mem. Natl Inst. Polar Res., Spec. Issue*, **22**, 125–139.
- OGAWA, T., BALSLEY, B. B., ECKLUND, W. L., CARTER, D. A. and JOHNSTON, P. E. (1982): Auroral radar observations at Siple Station, Antarctica. *J. Atmos. Terr. Phys.*, **44**, 529–537.
- RUMMER, W. D. (1968): Two-pulse spectral measurements. *Bell. Teloph. Lab. Rep.*, MM68–4121–15.

(Received November 14, 1981; Revised manuscript received December 14, 1981)